Anisotropic Light Transport in White Beetle Scales

Anisotropic Light Transport in White Beetle Scales

Lorenzo Cortese, Lorenzo Pattelli, Francesco Utel, Silvia Vignolini, Matteo Burresi, and Diederik S. Wiersma**

Rather than exploiting selective absorption by pigments, certain insects achieve coloration using complex photonic structures.[1–4] For instance, bright and iridescent colors are achieved by butterflies and beetles exploiting optical coherent effects in ultrathin periodic layers of low-refractive-index material[3,5,6] A bright white diffuse appearance is instead more complicated to achieve, since all colors have to be reflected with the same high efficiency. Since *broadband* high reflectance cannot be obtained with optical coherent effects (which would lead to wavelength dependencies and iridescence), bright whiteness is usually achieved with thick *disordered* systems which multiply scatter light. The lower the refractive index n of the scattering elements, the thicker the system has to be to achieve a pronounced brightness. The *Cyphochilus* beetle is an exception to this, since it obtains a remarkably brilliant white color with extremely thin scales, whose interior is made of a nanostructured random network of low-refractive-index chitin ($n = 1.56$).[7,8] In a recent study, we have shown that the multiple scattering of light occurring inside the scales is responsible of the bright broadband reflectance of this insect and that this scale is one of most strongly scattering low-refractive-index materials known.[9] We argued that their internal structure may have evolved, over millions of years,[4] toward optimal light scattering employing as little material as possible. We hypothesized that the apparent anisotropy of the chitin network could represent the crucial aspect of such scattering optimization.

In this work, we unequivocally demonstrate that the scales covering the *Cyphochilus*' body exhibit anisotropic light transport, which in turn comes as a direct consequence of the anisotropic arrangement and shape of the scatterers. Light transport in the scales thus has evolved to increment the scattering strength along the out-of-plane direction, leading to a pronounced total reflectance, i.e., its brightness. This led, as a trade-off, to a decrease of the in-plane scattering strength, which in any case does not contribute to the brightness. In this respect, our results identify the degree of anisotropy as a key microscopic structural feature in determining a bright white reflectance for thin, low-refractive-index optical coatings. Such discovery can be successfully applied in developing new lightweight, thin optical materials with immediate technological impact in applications ranging from coatings to displays and light-emitting diodes (LEDs)/illumination.

The structure responsible of the extraordinary bright whiteness of the *Cyphochilus* beetle is shown in **Figure 1**. The body of the beetle is covered by white scales (Figure 1b), which are about 100 µm wide and 250 µm long. Analysis on scanning electron microscope (SEM) images of 80 different scales of the same beetle, gently dissected with a razor blade, reveals an average thickness of 7 µm with a standard deviation of $\sigma = 1.5$ µm (**Figure 2**a). The bright whiteness of the *Cyphochilus* beetle scales angle results from multiple scattering of light by the microstructure present inside the scales (Figure 1d),[9] which is characterized by a cuticular random network of interconnected chitin rods, typically shorter than 1 µm and with a diameter of approximately 250 nm.[7] SEM images and analysis reported in literature reveal a very high filling fraction of the chitin network with respect to the volume of the scale ($f \approx 60\%$).[7,9]

As discussed in our previous work,[9] the particular morphology of the internal structure allows a high density of scatterers (which intuitively increases the scattering intensity and, consequently, the brightness) yet reducing the optical crowding effect (which instead tends to lower the overall scattering strength).[10] A high filling fraction usually leads to pronounced structural correlations due to the physical size of the scattering elements,[11,12] which in turn leads to a modulated spectral response, i.e., a coloration.[13–16] This is the case, for example, of the blue and green appearance of certain species of birds,[17–19] which is determined by the strong degree of spatial correlations in the structural disorder of their feathers. In contrast, the disorder in *Cyphochilus* scales has evolved in order to avoid spatial correlations, and yet maintain a high filling fraction, by exploiting the anisotropic shape of the scatterers. This comes to a cost: high packing fractions of rods can be reached only introducing a certain degree of angular correlations.[20] Indeed, from analysis of electron images of the interior of the white scales we can observe that the chitin rods appears to be mainly aligned with a planar orientation. As a consequence of such structural anisotropy, also light transport is expected to be anisotropic,

L. Cortese, L. Pattelli, F. Utel, Dr. M. Burresi, Prof. D. S. Wiersma
European Laboratory for Non-linear Spectroscopy (LENS)
Università di Firenze
Via Nello Carrara 1, 50019 Sesto Fiorentino, (FI), Italy
E-mail: cortese@lens.unifi.it; wiersma@lens.unifi.it
Dr. S. Vignolini
Department of Chemistry
University of Cambridge
Lensfield Road, Cambridge CB2 1EW, UK
Dr. M. Burresi
Istituto Nazionale di Ottica (CNR-INO)
Largo Fermi 6, 50125 Firenze, (FI), Italy
Prof. D. S. Wiersma
Department of Physics
Università di Firenze
Via Sansone 1, 50019 Sesto Fiorentino, (FI), Italy

DOI: 10.1002/adom.201500173

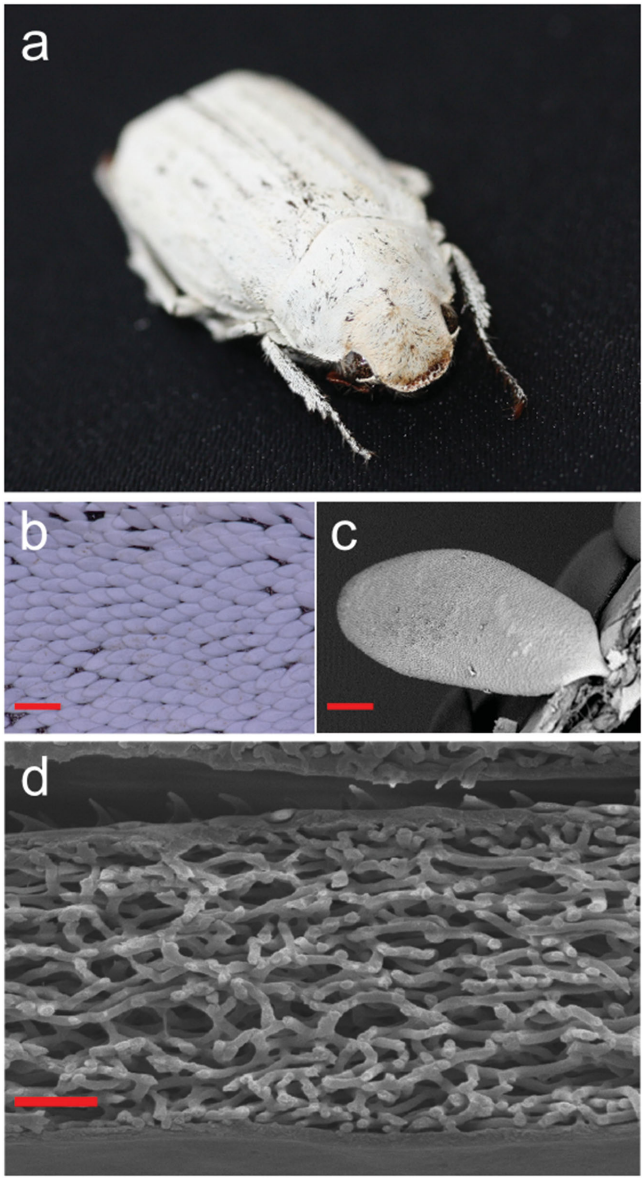

Figure 1. a) Image of *Cyphochilus*. b) Particular of the scales. c) SEM image of an entire scale. d) SEM image of a dissected scale. Scale bars: (b) 400 μm, (c) 25 μm, (d) 2μm.)

as observed in many structurally anisotropic materials such as biological tissues,[21,22] nematic liquid crystals,[23,34] or plastic porous fiber samples.[25,26] Therefore, a proper light transport investigation of the scales represents a powerful tool for a noninvasive study of their morphological anisotropy and from this shed light on the mechanism that leads to its bright white reflectance.

We revealed transport anisotropy combining the results of two independent steady state experiments performed on different scales. First, we measured the total transmission through a scale, which is an indirect measurement of the brightness in absence of absorption (this is the case of the beetle scales, as reported by Burresi et al.,[9] Supporting Information). Second, we performed steady state imaging of the diffuse light transmitted through the scale, which is strongly affected by the anisotropy of the system.[26–28] We demonstrated that the results of these two independent experiments are in contradiction when interpreted with isotropic diffusion theory. In contrast anisotropic theory, which accounts for different diffusion coefficients along different axes (see the Supporting Information), can perfectly reproduce the experimental data.[26,27] Since all the scales exhibit similar transport properties, we report here only the results relative to a single reference scale.

In case of negligible absorption, the measurement of the total transmission T_{tot} through a diffusive slab is an indirect estimation of the total reflectance R_{tot}, namely, of the brightness of the system. Isotropic diffusion theory relates the measured total transmission to the thickness t of the slab and the transport mean free path l_t, through the well known Ohm's law for light.[9] By neglecting absorption and ballistic light,[9] it can be written as:[29]

$$T_{tot} = \frac{l_t + z_e}{t + 2z_e} = \frac{1 + \frac{2}{3}A}{\mathrm{OT} + \frac{4}{3}A} \tag{1}$$

where $z_e = 2l_tA/3$ is the so-called extrapolation length[30] and A is a coefficient that takes into account the internal reflection due to the refractive index mismatch with the environment.[9,31] The OT is the optical thickness of the system and it is defined by the relation $\mathrm{OT} = t/l_t$. We calculated A as done by Burresi et al.,[9] by employing the phenomenological formula proposed by Contini et al.,[31] and applying the Maxwell Garnett mixing rule with a filling fraction of 0.61[9] to calculate the average refractive index of the scale. To measure the total transmission we focused a laser beam (wavelength 550 nm, focal spot diameter of 1.5 μm) on the central part of the scale, orthogonal to its surface, and we used an integrating sphere to collect all the light emerging from the scale (see figure in the Supporting Information). We measured $T_{tot} = 0.29 \pm 0.2$. This value is an average of several measurements made in a relatively small area in the central part of the scale, where it can be considered flat with a good approximation. For this reason, in this experiment, we neglected the actual smooth curvature of the scale toward its edges and we approximated it to a slab with an effective thickness. The obtained value of $\mathrm{OT} = 5.8 \pm 0.7$ is consistent with what reported in our previous study.[9] For this OT, considering a 2σ spanning range of thicknesses with respect to the center of the measured distribution (Figure 2a), the value of the transport mean free path results between 0.9 and 1.6 μm, confirming the fact that the *Cyphochilus* scale is one of the mostly scattering low-refractive-index system known.

Here we propose an independent way to retrieve the transport mean free path of a diffusive slab, by measuring the spatial transmission profile[32] $T(x,y)$ at the output surface (Figure 2b). It is well known that, according to diffusion theory, the full width of the "bell shaped" transmission profile is of the order of the sample thickness and barely affected by the transport properties. However, the exponential tails of such profile depend mostly on the transport mean free path l_t.[31] Thus accurate spatial measurements, with proper background subtraction and reduction of aberrations, can be used to infer the

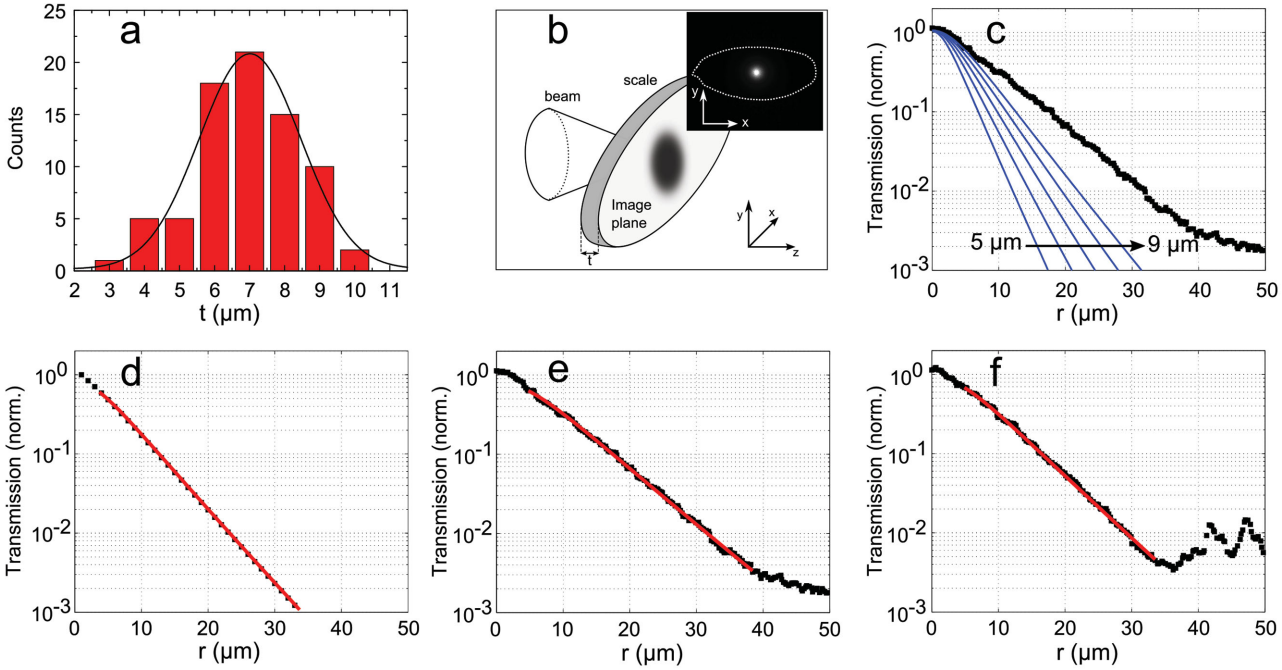

Figure 2. a) Thickness histogram obtained dissecting 80 different scales. Black line: Gaussian fit of the distribution. b) Geometric sketch of the experiment. Inset: an actual image of the spatial profile of the light transmitted through the scale as acquired by the camera; the dashed line is the contour of the scale. c) Crosscut along the *x* axis of the spatial transmission profile (experimental data). Blue lines: prediction of isotropic diffusion equation for OT = 5.8 and crescent thickness, from $t = 5$ μm to $t = 9$ μm, corresponding to a 2σ range with respect to the center of the distribution (a). d) Dots: Monte Carlo simulated spatial profile of an isotropic sample with OT = 5.8. Red line: fit with isotropic diffusion equation. e,f) Dots: crosscuts along *x* and *y* axes, respectively, of the spatial transmission profile (experimental data). Red line: fit curve obtained using the anisotropic diffusion equation.[27]

transport properties of the beetle's scales. Keeping the same experimental conditions as in the total transmission measurement, we focused a laser beam on the front side of the scale while imaging its back side on a CCD camera. Figure 2b shows the geometrical sketch of the experiment, with the image plane parallel to the *xy* plane and the beam direction parallel to *z* axis (see the Supporting Information for further details on the setup). The beam impinged in the central part of the scale, and we investigated a region of 40 μm radius centered in the beam focus, where we can consider the scale as a slab with an effective thickness. The resulting image (Figure 2b, inset) is an average of 20 different acquisitions taken moving the beam within a small central area of the scale. This procedure, together with a relatively broadband source ($\Delta\lambda = 10$ nm), makes the investigation statistically accurate, averaging over several realizations of disorder. We compared a crosscut of the imaged profile together with the prediction obtained from the isotropic diffusion equation[31] for the optical thickness measured with the total transmission experiment, that is, OT = 5.8. Thereafter, we also considered various physical thicknesses in a range of 2σ with respect to the center of the Gaussian distribution (Figure 2a). This analysis, reported in Figure 2c, clearly shows the discrepancy between the experimental data and the prediction according to isotropic diffusion theory.

The appropriateness of isotropic diffusion to describe light transport in such a thin system must be put to question, since its accuracy rapidly decreases for OT < 10.[33] Therefore we performed isotropic Monte Carlo simulations for a disordered slab with OT = 5.8 and the same effective refractive index of the scale. Figure 2d shows the simulated isotropic profile with an isotropic diffusion theory fit of the profile tail. Despite the low optical thickness the transport parameters are retrieved within an accuracy better than 1%, as long as the central points of the profile are excluded. This is necessary since ballistic and low order scattered light, which have a dominant contribution to the peak of the transmission profile in thin slabs, are not taken into account in the diffusion approximation.[34] We conclude that the large discrepancy shown in Figure 2c is not due to a possible breakdown of diffusion theory, but must be caused by the very nature of light transport in the scale (i.e., transport is not isotropic).

Encouraged by the anisotropy noticed in the electron images, we analyzed the results of the imaging and total transmission experiments in terms of anisotropic diffusion theory.[26–28,35,36] Anisotropic diffusion equation indeed links the transmitted light through a diffusive slab with its thickness and with the diffusion coefficients, and thus the transport mean free paths, along the different axes (see the Supporting Information).[27] It is fundamental to note that, in the case of anisotropic transport, the Ohm's law is still valid, provided that l_t in Equation (1) is replaced with the transport mean free path along the direction orthogonal to the scale surface (l_{tz} with the notations of Figure 2b). Hence, to increase the brightness is only necessary to decrease the mean free path along the *z*-direction, regardless of the in-plane properties.

Even in the anisotropic diffusion approximation, we can still define the optical thickness as $\mathrm{OT} = t/l_{tz}$ and determine it experimentally. As before, we considered a set of $l_{tz} = t/\mathrm{OT}$ values,

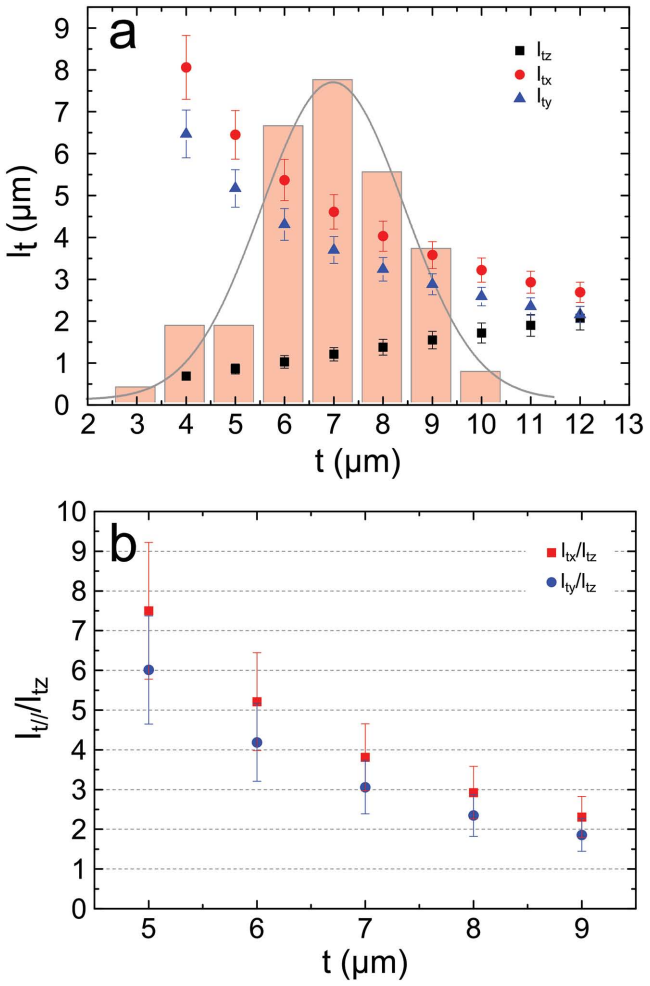

Figure 3. a) Values of l_t along the three different axes obtained fitting the transmission profiles with the anisotropic diffusion equation for fixed values of thickness chosen in a range compatible with the actual size of the scales. The graph is overlapped with the distribution of thickness. b) Ratio between l_t in the plane of the scale surface and l_t perpendicular to the scale surface. The results are displayed only for values of thickness in a range of 2σ with respect to the center of the distribution.

keeping OT = 5.8 constant and varying t in a 2σ range with respect to the center of the measured distribution. Then, we performed fits of crosscuts along the x and y axes of the imaged transmission profile using the anisotropic diffusion equation[27] (see the Supporting Information), with, respectively, l_{tx} or l_{ty} as the only fitting parameter. Examples of anisotropic fits are reported in Figure 2e,f for crosscuts along the x and y axes. The results of the fits for different thicknesses are plotted in **Figure 3**a,b (see Table 1 in the Supporting Information).

We found that l_{tx} and l_{ty} are always appreciably larger than l_{tz}. For thicknesses inside an interval larger than 2σ with respect to the center of the distribution the ratio between $l_{t//}$ and l_{tz} lays between 7 and 2. The plotted data suggest as well that l_{tx} (transport along the long axis of the scale) is slightly bigger than l_{ty} (short axis). This implies an in-plane anisotropy which seems to be plausible since the "growth" direction of the scales is along the x axis. However, we cannot make any definitive statement on the subject since the scales have a more pronounced curvature along the y-direction and this might create some reshaping in the transmitted profile. In contrast, the z-direction anisotropy of light transport is clearly evident, demonstrating that the anisotropy of the intrascale structure is optimized to increase the scattering along the direction normal to the scale surface. This come to the cost of a longer in plane transport mean free path, which however does not contribute to the brightness.

In conclusion, we unequivocally demonstrated that the scales of the *Cyphochilus* beetle show anisotropic light transport. This result has a general validity in that it has been inferred irrespective of the actual thickness of the investigated scale, i.e., over a wide range of possible values. The anisotropic transport is a fingerprint of the structural anisotropy of the intrascale chitin network, which optimizes light scattering to achieve a brilliant, white reflectance with a thin, lightweight structure. As a result of a long evolutionary process, *Cyphochilus* beetles indeed developed a dense, anisotropic network compressed along the direction orthogonal to the scale surface. This arrangement is optimized to selectively enhance the scattering strength in the normal direction, increasing the total reflectance, at expense of the scattering strength in the plane, which anyway is not relevant for the brightness.

Notably, optimizing angular correlations in network-like optical materials seems still a largely unexplored strategy in many applications. Considering, for example, the recently growing field of cellulose photonics, it is well known that for highly packed systems, moving from micrometric fibers (like common paper) to sub-μm fibrils leads to increased transparency.[37–39] On the contrary, we demonstrated that an optical system with analogue high density and low refractive index can exhibit an exceptional turbidity even with sub-μm scatterers, provided that its geometry is properly optimized. The range of optical applications that could profitably get inspiration from the scale's structure is widened by its extreme thinness and lightweight. Ultrathin diffuse reflector layers are relevant in enhancing the performances of LEDs[40] and displays,[41] while the broadband reflection capabilities of the anisotropic structure could find application both for UV-screening fabrics[42] as well as for IR-reflecting building thermoregulating coatings.[43]

Experimental Section

Total Transmission: The excitation was provided by a Fianium 1060 supercontinuum source. The beam was focused on the sample with a high NA aspheric lens (spot diameter in the focus ≈1.5 μm). The beam has been filtered with a bandpass filter with central wavelength of 550 nm and bandwidth of 10 nm. The scale was held (by electrostatic forces) on a ND 3 filter, to minimize the background light due to doubly reflected light, at the entrance port of an integrating sphere. The transmission at the output of the sphere was measured using a silicon photodiode and a lock-in amplifier.

Imaging of Transmission Profile: The excitation conditions were the same of the total transmission experiment. The beam was circularly polarized (we used a quarter-wave plate) to avoid polarization artifacts due to single scattering by anisotropic scatterers. The imaging part of the setup was composed by a 20× Olympus objective, a tube lens and an Andor Apogee cooled CCD camera. The scale was held (by electrostatic forces) on a ND 3 filter. The resulting image of the profile is an average of 20 different acquisitions.

Supporting Information

Supporting Information is available from the Wiley Online Library or from the author.

Acknowledgements

The authors wish to thank P. Vukusic for having provided the beetle's scales used in the experiments and U. Steiner for fruitful discussions. The research leading to these results has received from the European Research Council under the European Union's Seventh Framework Programme (FP7/2007–2013)/ERC Grant Agreement No. [291349] and the BBSRC David Phillips fellowship [BB/K014617/1].
The licence on this manuscript was changed after publication, on October 20, 2015.

Received: March 30, 2015
Revised: May 16, 2015
Published online: June 24, 2015

[1] P. Vukusic, J. R. Sambles, *Nature* **2003**, *424*, 852.
[2] M. Srinivasarao, *Chem. Rev.* **1999**, *99*, 1935.
[3] S. Kinoshita, *Structural Colors in the Realm of Nature*, World Scientific Publishing Co., Singapore **2008**.
[4] A. R. Parker, *J. Opt. A: Pure Appl. Opt.* **2000**, *2*, 15.
[5] P. Vukusic, J. R. Sambles, C. R. Lawrence, R. J. Wootton, *Proc. R. Soc. B* **1999**, *266*, 1403.
[6] D. G. Stavenga, B. D. Wilts, H. L. Leertouwer, T. Hariyama, *Proc. R. Soc. B* **2011**, *366*, 709.
[7] P. Vukusic, B. Hallam, J. Noyes, *Science* **2007**, *315*, 348.
[8] S. M. Luke, B. T. Hallam, P. Vukusic, *Appl. Optics* **2010**, *49*, 4246.
[9] M. Burresi, L. Cortese, L. Pattelli, M. Kolle, P. Vukusic, D. Wiersma, U. Steiner, S. Vignolini, *Sci. Rep.* **2014**, *4*, 6075.
[10] M. K. Gunde, Z. C. Orel, *Appl. Opt.* **2000**, *39*, 622.
[11] S. Torquato, F. H. Stillinger, *Rev. Mod. Phys.* **2010**, *82*, 2633.
[12] C. Song, P. Wang, H. A. Makse, *Nature* **2008**, *453*, 629.
[13] M. Reufer, L. F. Rojas-Ochoa, S. Eiden, J. J. Sáenz, F. Scheffold, *Appl. Phys. Lett.* **2007**, *91*, 171904.
[14] J. K. Yang, C. F. Schreck, H. Noh, S. Fatt Liew, M. I. Guy, C. S. O'Hern, H. Cao, *Phys. Rev. A* **2010**, *82*, 053838.
[15] S. Fatt Liew, J. K. Yang, H. Noh, C. F. Schreck, E. R. Dufresne, C. S. O'Hern, H. Cao, *Phys. Rev. A* **2011**, *84*, 063818.
[16] S. Magkiriadou, J. G. Park, Y. S. Kim, V. N. Manoharan, *Phys. Rev. E* **2014**, *90*, 062302.
[17] H. Noh, S. F. Liew, V. Saranathan, S. G. Mochrie, R. O. Prum, *Adv. Mater.* **2010**, *22*, 2871.
[18] H. Yin, B. Dong, X. Liu, T. Tianrong, L. Shi, J. Zi, E. Yablonovitch, *Proc. Natl. Acad. Sci. USA* **2012**, *109*, 10798.
[19] J. Tinbergen, B. D. Wilts, D. G. Stavenga, *J. Exp. Biol.* **2013**, *216*, 4358.
[20] S. R. Williams, A. P. Philipse, *Phys. Rev. E* **2003**, *67*, 051301.
[21] A. Kienle, F. K. Forster, R. Diebolder, R. Hibst, *Phys. Med. Biol.* **2003**, *48*, N7.
[22] T. Binzoni, C. Courvoisier, R. Giust, G. Tribillon, T. Gharbi, J. C. Hebden, T. S. Leung, J. Roux, D. T. Delpy, *Phys. Med. Biol.* **2006**, *51*, N79.
[23] D. S. Wiersma, A. Muzzi, M. Colocci, R. Righini, *Phys. Rev. Lett.* **1999**, *83*, 4321.
[24] M. H. Kao, K. A. Jester, A. G. Yodh, *Phys. Rev. Lett.* **1996**, *77*, 2233.
[25] P. M. Johnson, S. Faez, A. Lagendijk, *Opt. Express* **2008**, *16*, 7435.
[26] P. M. Johnson, A. Lagendijk, *J. Biomed. Opt.* **2009**, *14*, 05436.
[27] A. Kienle, F. Foschum, A. Hohmann, *Phys. Med. Biol.* **2013**, *58*, 6205.
[28] O. K. Dudko, G. H. Weiss, *Biophys. J.* **2005**, *88*, 3205.
[29] D. J. Durian, *Phys. Rev. E* **1994**, *50*, 857.
[30] R. C. Haskell, L. O. Svaasand, T. T. Tsay, T. C. Feng, M. S. McAdams, *J. Opt. Soc. Am. A* **1994**, *11*, 2727.
[31] D. Contini, F. Martelli, G. Zaccanti, *Appl. Opt.* **1997**, *36*, 4587.
[32] P. Barthelemy, J. Bertolotti, D. S. Wiersma, *Nature* **2008**, *453*, 495.
[33] R. Elaloufi, R. Carminati, J. Greffet, *J. Opt. Soc. Am. A* **2004**, *21*, 1430.
[34] T. J. Farrel, M. S. Patterson, B. Wilson, *Med. Phys.* **1992**, *19*, 879.
[35] E. Alerstam, *Phys. Rev. E* **2014**, *89*, 063202.
[36] A. Kienle, *Phys. Rev. Lett.* **2007**, *98*, 218104.
[37] M. Nogi, S. Iwamoto, A. N. Nakagaito, Y. Hiroyuki, *Adv. Mater.* **2009**, *21*, 1595.
[38] Z. Fang, H. Zhu, Y. Yuan, D. Ha, S. Zhu, C. Prston, Q. Chen, Y. Li, X. Han, S. Lee, G. Chen, T. Li, J. Munday, J. Huang, L. Hu, *Nano Lett.* **2014**, *14*, 765.
[39] V. Kumar, R. Bollström, A. Yang, Q. Chen, G. Chen, P. Salminen, D. Bousfield, M. Toivakka, *Cellulose* **2014**, *21*, 3443.
[40] H. Luo, J. K. Kim, E. F. Schubert, J. Cho, C. Sone, Y. Park, *Appl. Phys. Lett.* **2005**, *86*, 243505.
[41] G. Kim, *Eur. Polym. J.* **2005**, *41*, 1729.
[42] J. Yip, S.-P. Ng, K. H. Wong, *Text. Res. J.* **2009**, *79*, 771.
[43] A. Synnefa, M. Santamouris, I. Livada, *Sol. Energy* **2006**, *80*, 968.